Studii şi Cercetări Ştiinţifice 2017, **18** (2), pp. 153 – 165
Chimie şi Inginerie Chimică, Biotehnologii, Industrie Alimentară

Scientific Study & Research
Chemistry & Chemical Engineering, Biotechnology, Food Industry *ISSN 1582-540X*

ORIGINAL RESEARCH PAPER

INVESTIGATION OF UV/TiO_2-ZnO-Co PHOTOCATALITIC DEGRADATION OF AZO DYE (REACTIVE RED 120) BY RESPONSE SURFACE METHODOLOGY

Mohsen Mansouri[1*], Marjan Tanzifi[1], Hossein Lotfi[2, 3], Mohsen Nademi[3]

[1]Ilam University, Department of Chemical Engineering, Ilam, Iran
[2]Institute for Color Science and Technology, Department of Environmental Research, Tehran, Iran
[3] Islamic Azad University North Tehran Branch, Department of Chemical Engineering, Tehran, Iran

*Corresponding author: mansouri2010@yahoo.com; m.mansouri@ilam.ac.ir

Received: January, 23, 2017
Accepted: June, 06, 2017

Abstract: Advanced oxidation processes (AOPs) are the most attractive methods to degrade diferent organic pollutants. The AOPs have grown extensively because water quality control and regulations have become very strict in many countries. Optimizing the photocatalytic degradation of azo dye (Reactive Red 120) was our goal of research for applying the experimental design methodology. *p*H (X_1), concentration of dye (X_2) and TiO2-ZnO-Co nanoparticles volume (X_3) in reactions were described mathematically as the function of parameters and were designed by using response surface methodology (RSM). Results were in agreement with empirical values and the sensitivity analysis showed above parameters as the most efficient variables in decolorization efficiency. Analysis of variance (ANOVA) revealed highly determination coefficient value (R^2 = 0.9996 and *adjusted*-R^2 = 0.999) and satisfactory prediction second-order regression model. The desirable quantities were obtained at the *p*H = 7, TiO_2-ZnO-Co concentration = 0.1 $g \cdot L^{-1}$, and the initial Reactive Red 120 (RR 120) concentration = 16.4 $mg \cdot L^{-1}$. Finally, kinetics reaction of degradtion RR 120 was carried in the optimum conditions.

Keywords: *Photocatalytic degradation, RR 120, TiO_2-ZnO-Co nanoparticles, response surface modelling*

INTRODUCTION

Azo dyes, which include one or more azo bond (-N=Ne-), are used for 60 - 70 percent of all textile pigments [1]. Other functional groups describing this class of complex are also the auxochromes such as -NH_2, -OH, -COOH, -SO_3H that used for the increase of the coloring tensity and the affinity with fibers [2]. It seems that approximately 10 - 15 % of total dye stuffs productions are destroyed in synthesis and dyeing processes [3]. Reactive dyes showed a great domain of various chemical structures, primarily based on alternative aromatic and heterocyclic groups. Removal of reactive dyes is difficult using common coagulation and activated sludge processes because of their high solubility in water [4]. Recently, different waste water treatment methods were used to prevent the aggregation of toxic dyes in the environment including: electro-flotation, membrane filtration, electro-coagulation, ion exchange, irradiation, etc. [5, 6]. Advanced oxidation process (AOP) is one of the suitable techniques for washing the organic dyes by heterogeneous semiconductor photocatalysts that in this method hydroxyl radicals (OH) are effective oxidizing successor for photocatalytic decolorization of Azo dyes [1 – 4]. AOPs involve chemical, photochemical or electrochemical processes leading to chemical degradation of organic pollutants [7]. Electro-Fenton (EF) and photoelectro-Fenton (PEF) methods are more popular AOPs techniques for removal of toxic organic pollutants. ZnO has been used successfully as a photocatalyst for achromatizing dye impurities between all semiconductors used in AOPs [8, 9]. Titanium dioxide (TiO_2) is one of the most favorable catalysits that is widely applied for destroying organic pollutant photocatalytically in water and air due to its advantages such as high photocatalytic activity, non-soluble, non-toxic, and low production cost, but it has a major disadvantage in its re-combination between electron and hole when it used purely. Several metal or nonmetal iron doping studies were done to smooth the way for improving the photocatalytic efficacy of TiO_2 [1, 3, 10 – 12]. Another noticeable problem is that technical advance related to progress of photocatalytic process has not been done completely. Various variables in this system should be considered and appraised. One of dams in this direction to use AOP in large scale is that in previous works One-factor-at-a-time (OFAT) was widely used [13, 14]. If this method is used, the checking between variables of operation process is not possible. In addition, considering indicates that this method is a time-consuming way and expensive method related to consuming chemical material [15]. Recently, many studies have been done to substitute more effective way such as Response Surface Methodology (RSM) for One-factor-at-a-time method. This method has been founded based on analysis, experimental design, and statistical explanation, which is a good strategy to determine the optimal condition in multiple variables systems. In this work, the removal of an Azo dye (Reactive Red 120) from aqueous solution using the photocatalyst semiconductor ZnO-Co supported on TiO_2 was studied. To investigate the influences of experimental parameters on the removal efficiency of RR 120, the response surface method was served. reasonably, efficacy of removing the stain was the desirable response and the experimental design determined the relation between response and significant factors that is a suitable instrument for optimizing processes [16].

MATERIALS AND METHODS

Materials

For the purpose of synthesis, hydroxyl propyl cellulose (HPC), titanium tetraisopropoxide (TTIP), acetic acid, pure ethanol, $Co(NO_3)_2 \cdot 6H_2O$, di-ethanol amine, ethanolamine, $Zn(NO_3)_2 \cdot 6H_2O$, NaOH and H_2SO_4 , Methyl tert-butyl ether (99.9 %)– all in analytical grade - are purchased from Merck Company.

Instruments

To determine nanoparticles' structure, XRD (Philips PW 1800) was employed. For identification of nanoparticles' surface morphology, the scanning electron microscope (SEM) (Leo 1455 VP) was used. UV-Vis spectrophotometer (Model T80+, PG Instruments, UK) machine measured the RR 120 concentrations.

Preparation of nanocatalyist

For synthesis of TiO_2-ZnO-Co nanocomposite, each part of it should be prepared separately before mixing by sol-gel method. In the following, the method of constructing of each component of nanocomposite will explain.
For preparing of TiO_2, at the first, hydroxyl propyl cellulose (HPC) was solved in ethanol under quick stirring for five minutes. Secondly, titanium tetra isopropoxide (TTIP) was added to previous mixture and was stirring for fifteen minutes. Third, the complex of glacial acetic acid, pure alcohol and deionized water was shed to previous mixture. Finally, it was shaked for fifteen minutes just to make sure that a yellow transparent acidic TiO_2 solution has been prepared. The sol was kept at room temperature for thirty minutes.
Second component of nanocomposite is ZnO. Firstly, Zinc nitrate hexahydrate was solved in net alcohol and was shaked for five minutes. Secondly, the solution of di-ethanol amine, pure alcohol, and deionized water was shed to solution under intensive constant stirring condition. Finally, the solution was continuously stirred for fifteen minutes to reach a transparent solution of ZnO.
Third component of nanoparticle is CoO. To beginning, cobalt nitrate hexahydrate was solved in the pure alcohol and mixed for five minutes. Then, the mixture of ethanolamine, sheer alcohol and distillated water was poured to solution under sever constant mixing condition. The solution was steadily mixed for fifteen minutes to reach an alkalinity transparent sol Co.
Finally, the sol of ZnO, and Co were shaked with the sol of TiO_2 directly to obtain the TiO_2-ZnO-Co nanocomposite. This nanocomposite was dried at room temperature. Then, the nanocomposite firstly was sintered at 350 °C for 10 minutes and after that, sintered at 500 °C for five hours in order to calcinate it (temperature was being increased 5 °C /s) finally, the nanocatalyst was obtained.

Experimental

All photochemical reactions for destruction of RR 120 with TiO_2-ZnO-Co were fulfilled in a batch reactor made from cylindrical glass with three litters in volume. The plan of reactor which used in this research is shown in Figure 1. Reaction mixture in the reactor circulates in the closed loop between pump and reactor. In addition, reactions' temperature was monitored. Three 15 W lamps from Phillips emitting UV light of wavelength 254 nm, which was soaking in the solution, was used to serve the UV radiation in reactor. 3 L of reaction mixture were used for each of the tests that proposed by RSM experimental design.

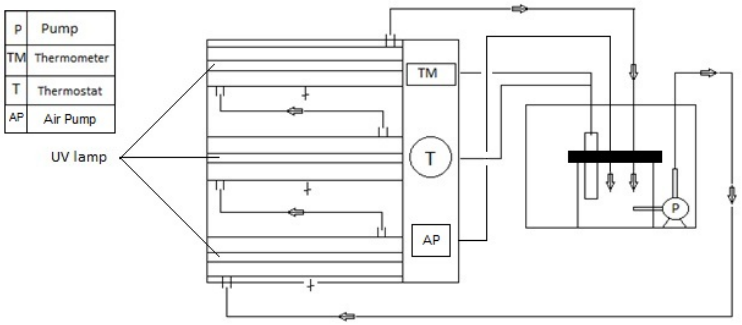

Figure 1. *Scheme of the reactor used in this study is represented*

Analysis

Removal of RR 120 was measured by UV-Vis spectrophotometer device. The RR 120 removal percent was obtained using Equation 1:

$$\text{RR 120 removal}(\%) = \frac{C_0 - C_t}{C_0} \times 100 \quad (1)$$

where C_0 is the primary concentration of RR 120 in ppm and C_t is RR 120's concentration based on ppm at any time *t*.

Experimental design and statistical analysis

Firstly, preliminary experiments were performed using single factor study method to specify the significant experimental parameters affecting the photocatalytic RR 120 treatment. Selected factors were catalytic dose, primary concentration of RR 120 and *p*H of reaction mixture.

To optimize the response, three selected experiential parameters were employed by RSM as the independent variables and the percentage of degradation of RR 120 as the dependent variables. Box– Behnken design of tests is used to examine the combined effects of three independent variables on the response through 15 sets of experiment. The ranges and levels of the independent variables are shown in Table 1. Box–Behnken plan is executed because it is highly effective and involve no point at the peaks of the cubic region modeled by the upper and lower limits of variables.

Table 1. *The levels and ranges of variables in Box–Behnken statistical experiment design*

Independent variables	Symbol	Coded variable level		
		low	center	high
		-1	0	+1
*p*H	A	4	7	10
Dye concentration [mg·L^{-1}]	B	10	20	30
Catalytic loading [g·L^{-1}]	C	0.08	0.1	0.12

This plan with RSM has been widely used to improve different physical, chemical and biological processes [17 – 19]. Using RSM, the results are matched to an experimental quadratic polynomial model for the three parameters showed in the Equation 2:

$$Y=\alpha_0+\alpha_1A+\alpha_2B+\alpha_3C+\alpha_{11}A^2+\alpha_{22}B^2+\alpha_{33}C^2+\alpha_{12}AB+\alpha_{23}BC+\alpha_{13}AC \quad (2)$$

Here, Y indicated the dependent variable, α_0 is the intercept, α_1, α_2 and α_3 are the coefficients of the independent variables, α_{11}, α_{22} and α_{33} are quadratic coefficients, α_{12}, α_{23} and α_{13} the interaction coefficients and A, B, C are the independent variables. Multiple regression analysis and optimization process were done by RSM and using Design Expert software (version 7, Stat Ease Inc., USA). The obtained values from analysis of variance (ANOVA) were found significant at $p < 0.05$. Three dimensional response surface analysis of the independent and dependent variables were used to find the desirable amounts for independent variables. Designed experiments and the real and predicted values of the response were represented in detailed in Table 2 and Figure 2. Effect of independents variable on the decomposition of RR 120 were shown in Figure 3 (a, b, c).

Table 2. *Box–Behnken experiments along with actual and predicted values of responses*

Run	A, *p*H	B, Dye concentration [mg·L^{-1}]	C, Catalyst loading [g·L^{-1}]	Dye removal [%]	
				Actual	Predicted
1	10	20	0.08	56.5600	56.489
2	4	20	0.12	56.3600	56.431
3	4	10	0.1	81.6000	81.174
4	7	30	0.12	71.4400	71.150
5	7	20	0.1	86.7600	86.487
6	10	20	0.12	62.3700	62.234
7	7	20	0.1	86.1700	83.730
8	7	20	0.1	86.5300	86.487
9	10	30	0.1	66.0450	66.471
10	4	20	0.08	48.1000	48.236
11	7	10	0.08	85.6200	85.910
12	7	10	0.12	90.3500	90.705
13	7	30	0.08	62.3600	62.005
14	4	30	0.1	57.7877	58.007
15	10	10	0.1	86.9833	86.764

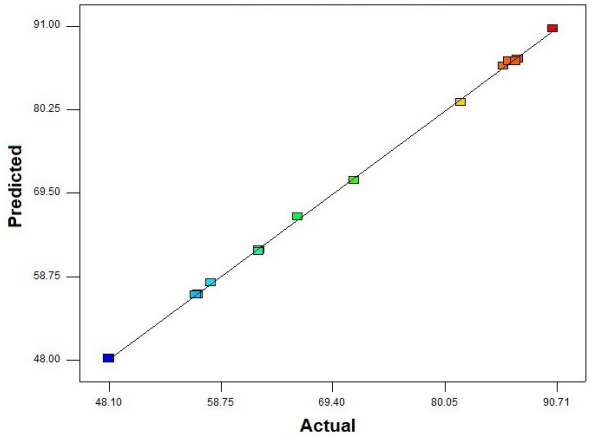

Figure 2. *Plot of the actual and predicted values for degradation of RR 120*

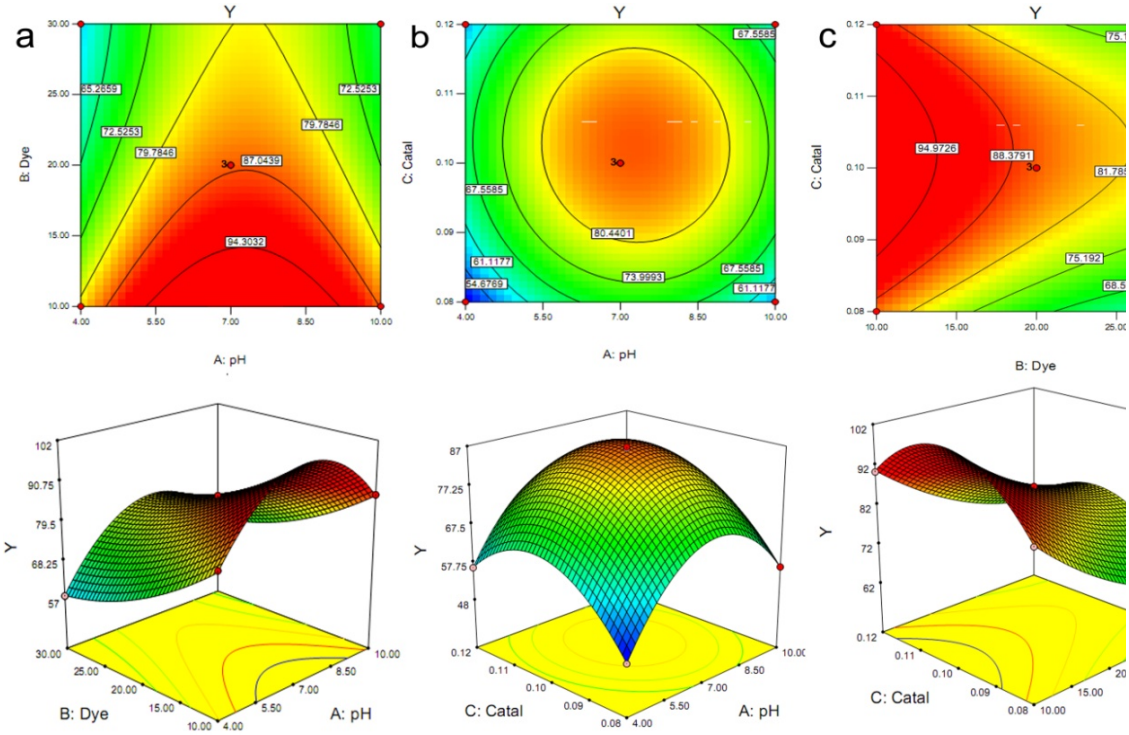

Figure 3. *Contour and surface plots of RR 120 removal (%) in uncoded values for t = 90 min.: (a) A (pH) and B (Dye) in fixed C (catalyst concentration) at 0.1 g·L^{-1}, (b) A (pH) and C (catalyst concentration) in fixed B (Dye) at 20 mg·L^{-1}, (c) B (Dye) and C (catalyst concentration) in fixed A (pH) at 7*

RESULTS AND DISCUSSION

Characterization of photocatalysts

In order to identify the skeleton of prepared TiO_2-ZnO-Co and TiO_2 nanoparticles that were presented in Figure 4a, the X-ray diffraction (XRD) was used. Based on the Figure 4a, it seems that all peaks are found at 25.38°, 37.94°, 48.04°, 54.69° and 62.93°

for TiO_2; and 25.26°, 37.98°, 47.97°, 53.56° and 62.53° for TiO_2-ZnO-Co. It is revealed that the 2 Theta values of X-ray patterns of TiO_2 and TiO_2-ZnO-Co compatible with anatase for both of them. The XRD patterns illustrate that the composition of TiO_2-ZnO-Co does not change the catalyst structure of TiO_2. This may result from the low concentration of Co and ZnO in the composition was low. Debye-Scherrer formula can measured the size of particles of samples (Equation 3):

$$D = \frac{K\lambda}{\beta \cos\theta} \tag{3}$$

In Equation 3, D is the mean of crystal size (nm), K is the Scherrer constant, an arbitrary value that comes down in the range 0.9 in current research, λ is wavelength of X-ray radiation (0.154 nm), θ is the diffraction angle and β is whole width at half maximum (FWHM). The particle size calculated value for TiO_2 and TiO_2-ZnO-Co nanoparticles is 11.81 nm and 11.76 nm, respectively.

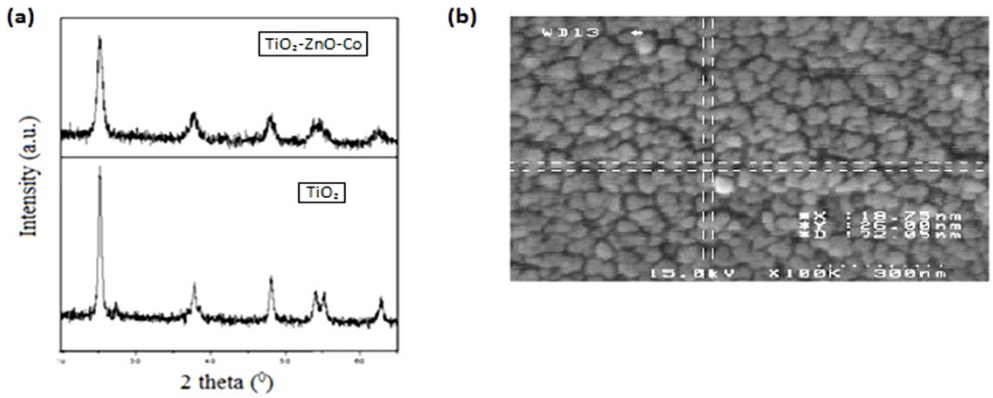

Figure 4. *Catalyst characterization (a) XRD pattern of TiO_2 and TiO_2–ZnO-Co, (b) SEM image of TiO_2–ZnO-Co*

Scanning electron microscope (SEM) was used to show the morphology of surface's samples that were prepared in this study, which is presented in Figure 4b. This figure revealed that sphere-shaped components are formed in good resemblance to each other. Based on the SEM Images, it is showed that the mean of particle size of TiO_2-ZnO-Co nanoparticles is almost 14.75 nm. In addition, it can be showed that there is a difference between crystal size measured by XRD and SEM. This difference can be derived from this fact that the result of an XRD pattern shows the crystal size of a particle, whereas the corollary of a SEM image represents the particle size itself which is the accumulation of several crystals [20].

Response surface methodology using for optimization of removal conditions

In order to achieve a suitable model, significance experiment has been done. Also for regression model and each coefficient of the model the test of lack-of-fit ought to be performed. The summary of test results listed in a common ANOVA table. Using ANOVA and the experimental information for destruction of RR 120 was statistically analyzed. These results are listed in Tables 2 - 4.

Table 3. *ANOVA for Response Surface Reduced Quadratic Model-Analysis of variance table*

Source	Sum of Squares	Degrees of freedom	Mean Square	F Value	P-value Prob> F	
Model	2943.50	9	327.06	1481.81	< 0.0001	significant
Residual	1.10	5	0.22			
Lack of fit	0.93	3	0.31	3.49	0.2305	not significant
Pure error	0.18	2	0.088			
Cor total	2944.61	14		R-Squared	0.9996	
				Adj R-Squared	0.9990	
				Adeq Precision	110.714	

Table 4. *ANOVA results for the coefficients of quadratic model for dye removal*

Factor	Coefficient estimate	Pareto analysis [%]	Standard error	95 % confidence interval low	95 % confidence interval high	F-value	p-Value
Intercept	86.49	-	0.27	85.79	87.18	-	-
A-*p*H	3.51	1.92	0.17	3.09	3.94	447.53	<0.0001
B- Dye	-10.87	18.45	0.17	-11.29	-10.44	4278.81	<0.0001
C-Catalyst	3.48	1.89	0.17	3.06	3.91	440.22	<0.0001
AB	0.72	0.081	0.23	0.11	1.32	9.36	0.0281
AC	-0.61	0.058	0.23	-1.22	-0.0080	6.80	0.0478
BC	1.09	0.19	0.23	0.48	1.69	21.43	0.0057
A^2	-17.49	47.77	0.24	-18.12	-16.86	5116.68	<0.0001
B^2	4.11	2.64	0.24	3.48	4.73	282.06	<0.0001
C^2	-13.15	27.0	0.24	-13.78	-12.52	2892.96	<0.0001

Obtained R-square is found to be 0.9996, which is near to 1 and significant, means that about 99.96 % of changes in the data can be explained by the model. The comparison between the range of the estimated value at design points with the mean prediction error is done by sufficient accuracy. The result of above comparison is obtained greater than 4 (110.714), implying the model's adequate discrimination power. Lack-of-fit P- value of 0.2305 shows the lack-of-fit is not meaningful ratio to pure error; this is suitable, since we look for a pattern that matches.

Following the empirical plan (Table 2), experiential second order polynomial equations are prepared for the degradation percent of RR 120 in terms of three independent variables as it is revealed in Equation 4.

$$\text{RR 120 removal} = +86.49 + 3.51\,A - 10.87\,B + 3.48\,C - 17.49\,A^2 + 4.11\,B^2 - 13.15\,C^2 + 0.72\,AB - 0.61\,AC + 1.09\,BC \quad (4)$$

ANOVA test of the second order polynomial model (F-value = 1481.81, p-value < 0.0001) revealed that the model is meaningful, i.e. 0.01 % for probability of the model's F value due to the noise. Due to the regression model's coefficient of degradation of RR 120, ANOVA is demonstrated in Table 4 as an additional tool to check the ultimate model's adequacy. To achieve a better commentary of the results, it was applied the Pareto analysis for computation of the percentage effect of each factor on the response as shown in Equation 5. [21]:

$$P_i = \left(\alpha_i^2 \Big/ \sum \alpha_i^2 \right) \times 100 \qquad i \neq 0 \tag{5}$$

As shown in Table 4, the variables that are more effective on the yield of decolorization were obtained to be initial solution concentration (α_2, 18.45 %), quadratic terms of *p*H (α_{11}, 47.77 %) and catalyst concentration (α_{33}, 27.0 %). Initial solution concentration of dye had negative effects on dye removal efficiency, but *p*H and TiO_2-ZnO-Co amount had positive effects on it.

The normal possibility plan (Scatter Diagram) for the studentized remaining is shown in Figure 5a. The points on this plan lie logically close to the direct line revealed that the errors have normal distribution with an average zero and a constant. The curvature P-value < 0.0001 showed that there is a considerable curvature (as calculated by the difference between the average score center and the mean factorial points) in the design space. Consequently, a linear model accompanied with the terms of engagement giving a twisted plane was not sufficient to explicate the response. Likewise, pieces of the residuals in Figure 5b represent that they have not any clear pattern and their skeleton is relatively abnormal. Additionally, they show identical scatter top and bottom the x-axis, indicating the suggest model's sufficiency, so there is not any reason to suspect any infringement. The optimal conditions for the maximum destruction of RR 120 were represented in Table 5.

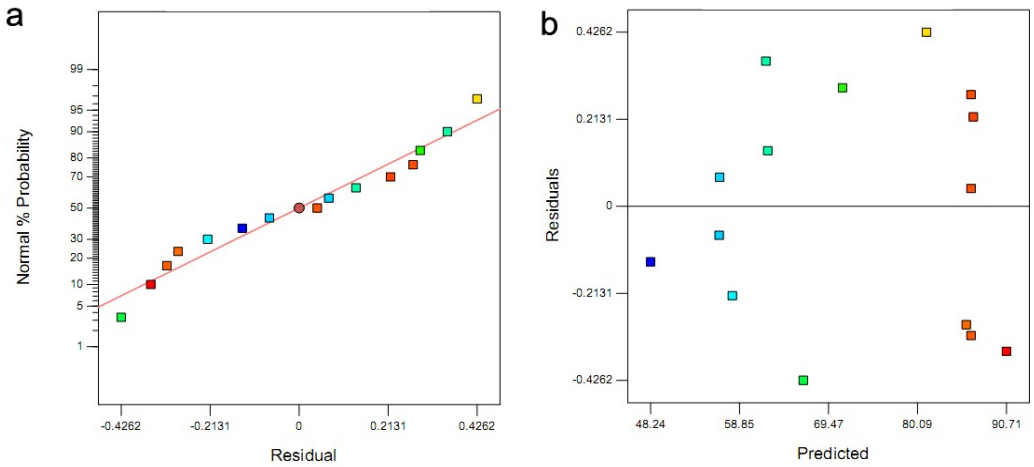

Figure 5. *(a) Normal probability plot of residual for degradation efficiency (%) (b) plot of residual and predicted values for degradation of RR 120*

Table 5. *The Optimum conditions selected for the maximum possible Dye removal, [%]*

A- *p*H	B- Dye Concentration [mg·L^{-1}]	C- catalytic dose [g·L^{-1}]	Dye removal [%] (predict)	Dye removal [%] (actual)
7	16.4	0.1	91.0987	88.994

Effect of effective variables on the Photocatalysis of RR 120

One of the most important variables in photocatalytic destruction of organic pollutant is *p*H. Effects of *p*H on photocatalytic destruction of RR 120 were examined with the

initial *p*H at three different values of 4, 7 and 10, as it is shown in Figure 6a. The destruction of RR 120 raises as the *p*H of solution increases from 4 to 7. Then, the RR percentage 120 degradation declines where as solution's *p*H value raises from 7 to 10. The *p*H of solution has sophisticated affects on the reaction of photocatalytic oxidation. Generally, the *p*H effect depends on type of pollution and zero point charge (ZPC) of semiconductor (catalyst) in process of oxidation. The phenomena can be stated in terms of the location of the point of zero charge (isoelectric point) of the TiO_2-ZnO-Co. It can be concluded based on results that obtained from Figure 3, *p*H 7 is the best value for destruction of RR 120 under above condition.

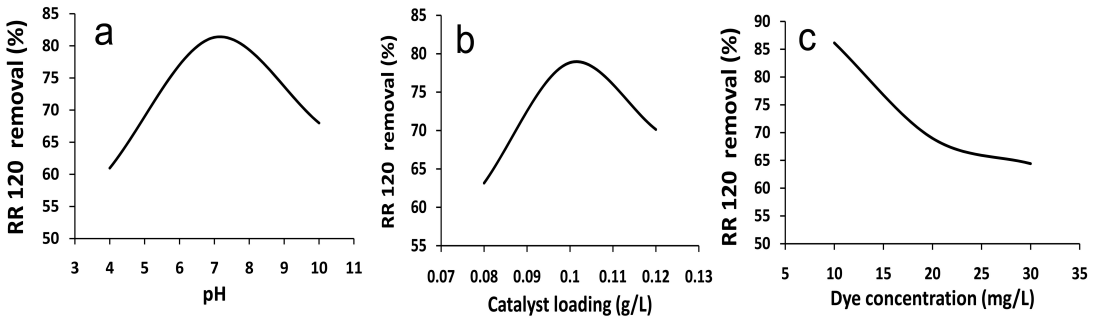

Figure 6. *Effect of pH, initial RR 120 concentration and catalytic dose on degradation efficiency [%]: (a) initial RR 120 concentration = 20 mg·L^{-1}; catalytic dose = 0.1 g·L^{-1}, (b) pH = 7; initial RR 120 concentration = 20 mg·L^{-1}, (c) pH = 7; catalytic dose = 0.1 g·L^{-1}.*

The tests were conducted to evaluate the effect of catalyst loading on photocatalytic destruction RR 120 under conditions 0.08, 0.1 and 0.12 g·L^{-1} of catalyst loading. Figure 6b shows the percentage of degradation efficacy versus catalyst loading for several initial TiO_2-ZnO-Co nonoparticles' concentrations. Based on the Figure 6b, it is obvious that the efficiency of degradation percent increase as the catalyst loading raises from 0.08 to 0.1 g·L^{-1}. However, this trend reverses and the percentage of degradation RR 120 goes down as catalyst loading is increased from 0.1 to 0.12 g·L^{-1}. Since the amount of catalyst increases, adsorbed photons and molecules number raises as well due to grow in the number of TiO_2-ZnO-Co nanoparticles. In result, the particles' value increases within the illumination area [22]. This reaction can be cited that some photocatalyst particles may not take sufficient energy to produce hydroxyl radical and start the oxidation of RR 120 [17]. It may also drive from TiO_2-ZnO-Co accumulation, increasing ambiguity, reducing the active points on its surface to absorb organic particles and UV, so decline the quantity of $e^- - h^+$ (electron-hole pair) and OH free radicals and influencing the destruction [17 – 19].

The effect of various primary concentrations of RR 120 solution on destruction of RR 120 was experimented, which results of this test were represented in Figure 6c. According to Figure 6c, it is obvious that increasing of primary concentration of RR 120 leads to less degradation of RR 120. Similar outcomes have been represented on the photocatalytic oxidation of other organic materials connection [17, 23]. Therefore, at low concentration of RR 120, a rapid destruction RR 120 results from a greater number of water molecules that will be absorbed onto the accessible TiO_2-ZnO-Co components, hydroxyl radicals production. In other world, in a high concentration of RR 120, there is a smaller piece of water molecules to free active sites, because the number of active

sites remains identical. In conclusion, it toughen up the rivalry between the RR 120 and water molecules to absorb on the catalyst, leads to drop in the destruction ratio.

Photocatalytic reaction kinetic

Based on optimal conditions which were achieved from former sections, the kinetic of photocatalytic destruction of the RR 120 was evaluated which is shown in Figure 7 at catalyst concentration of 16.4 mg·L^{-1}, and under light intensity 15 W UV-C. Overall, first-order kinetic is appropriate for photocatalytic reactions [12]. Kinetic model as follows:

$$-r_A = -\frac{dC}{dt} = K\,C \tag{6}$$

After integration of Equation (7), the bellow equation is obtained:

$$Ln\left(\frac{C_0}{C}\right) = K\,t \tag{7}$$

Here the r_A is the oxidation ratio of the RR 120 (ppm·min^{-1}), K the appearance constant of the reaction rate (the constant of first order reaction), C the concentration of the RR 120 (ppm), C_0 the initial concentration of RR 120, t the time required for primary concentration of RR 120 C_0 to become C (min).

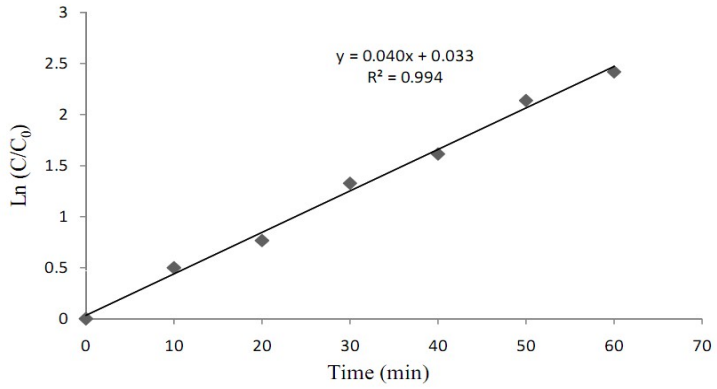

Figure 7. *Kinetic of RR 120 degradation under UV irradiation based on optimum conditions*

The gradient of the Ln (C_0 /C) against time pieces under optimized conditions shows the constant ratio of degradation RR 120. Amounts of the first-order destruction constants (K) similar to the linear regression (R^2) values are represented in Table 6.

Table 6. *Optimum conditions and kinetic constant of RR120 degradation*

A- *p*H	B- initial Dye Concentration [mg·L^{-1}]	C- catalytic dose [g·L^{-1}]	R^2	K_{app} [min^{-1}]
7	16.4	0.1	0.9953	0.0497

CONCLUSIONS

The optimization and the modelling of photocatalytic destruction of azo dye (Reactive Red 120) were done using a composite empirical design. The mathematical model could predict the photocatalytic degradation at any point in the experimental domain subsequently similar to set off the optimum degradation conditions. The high relevance in the model shows that the second-order polynomial model could be used to optimize the photocatalytic destruction of dye. The conditions to get 91.09 % for reaction to decolorization were obtained to be *p*H (X_1) = 7, amount of RR 120 dye (X_2) = 16.4 $mg \cdot L^{-1}$, and TiO_2-ZnO-Co concentration (X_3) = 0.1 $g \cdot L^{-1}$. A relatively high specification coefficient (R^2 = 0.9996, Adj-R^2 = 0.999) achieved via analysis of variance (ANOVA) represented an acceptable agreement of the prediction model with the empirical values, and the most efficient variables on the decolorization efficiency were achieved to be primary solution concentration, quadratic terms of *p*H and catalyst concentration.

REFERENCES

1. Muruganandham, M., Swaminathan, M.: Solar photocatalytic degradation of a reactive azo dye in TiO_2-suspension, *Solar Energy Materials and Solar Cells,* **2004, 81** (4), 439-457;
2. Molinari, R., Pirillo, F., Falco, M., Loddo, V., Palmisano, L.: Photocatalytic degradation of dyes by using a membrane reactor, *Chemical Engineering and Processing,* **2004**, **43** (9), 1103-1114;
3. Konstantinou, I.K., Albanis, T.A.: TiO_2-assisted photocatalytic degradation of azo dyes in aqueous solution: kinetic and mechanistic investigations. A review, *Applied Catalysis B: Environmental,* **2004**, **49** (1), 1-14;
4. Akyol, A., Yatmaz, H.C., Bayramoglu, M.: Photocatalytic decolorization of Remazol Red RR in aqueous ZnO suspensions, *Applied Catalysis B: Environmental* **2004**, **54** (1), 19-24;
5. Xie, Y.B., Li, X.Z.: Interactive oxidation of photoelectrocatalysis and electro-Fenton for azo dye degradation using TiO_2–Ti mesh and reticulated vitreous carbon electrodes, *Materials Chemistry and Physics,* **2006**, **95** (1), 39-50;
6. Rauf, M.A., Salman Ashraf, S.: Fundamental principles and application of heterogeneous photocatalytic degradation of dyes in solution, *Chemical Engineering Journal,* **2009**, **151** (1-3), 10-18;
7. De-Laat, J., Gallard, H.: Catalytic decomposition of hydrogen peroxide by Fe(III) in homogeneous aqueous solution: Mechanism and kinetic modeling, *Environmental Science & Technology,* **1999**, **33** (16), 2726-2732;
8. Khodja, A.A., Sehili, T., Pilichowski, J.F., Boule, P.: Photocatalytic degradation of 2-phenylphenol on TiO_2 and ZnO in Aqueous Suspensions, *Journal of Photochemistry and Photobiology A: Chemistry,* **2001**, **141**, 231-239;
9. Moradi, H., Sharifnia, S., Rahimpour, F.: Photocatalytic decolorization of reactive yellow 84 from aqueous solutions using ZnO nanoparticles supported on mineral LECA, *Materials Chemistry and Physics,* **2015**, **158**, 38-44;
10. Liqiang, J., Honggang, F., Baiqi, W., Dejun, W., Baifu, X., Shudan, L., Jiazhong, S.: Effects of Sn dopant on the photoinduced charge property and photocatalytic activity of TiO_2 nanoparticles, *Applied Catalysis B: Environmental,* **2006**, **62** (3-4), 282-291;
11. Luo, H., Takata, T., Lee, Y., Zhao, J., Domen, K., Yan, Y.: Photocatalytic activity enhancing for titanium dioxide by Co-doping with bromine and chlorine, *Chemistry of Materials,* **2004**, **16** (5), 846-849;
12. Safari, M., Nikazar, M., Dadvar, M.: Photocatalytic degradation of methyl tert-butyl ether (MTBE) by Fe-TiO_2 nanoparticles, *Journal of Industrial and Engineering Chemistry* **2013**, **19** (5), 1697-1702;

13. Toor, A.P.: Photocatalytic degradation of direct yellow 12 dye using UV/TiO_2 in a shallow pond slurry reactor, *Dyes and Pigments,* **2006**, **68** (1), 53-60;
14. Chin, S.S., Lim, T.M., Chiang, K., Fane, A.G.: Factors affecting the performance of a low-pressure submerged membrane photocatalytic reactor, *Chemical Engineering Journal,* **2007**, **130** (1), 53-63;
15. Sakkas, V.A., Islam, M.A., Stalikas, C., Albanis, T.A.: Photocatalytic degradation using design of experiments: A review and example of the Congo red degradation, *Journal of Hazardous Materials,* **2010**, **175** (1-3), 33-44;
16. Khataee, A.R., Zarei, M., Moradkhannejad, L.: Application of response surface methodology for optimization of azo dye removal by oxalate catalyzed photoelectro-Fenton process using carbon nanotube-PTFE cathode, *Desalination,* **2010**, **258** (1), 112-119;
17. Zhang, J., Fu, D., Xu, Y., Liu, C.: Optimization of parameters on photocatalytic degradation of chloramphenicol using TiO_2 as photocatalyist by response surface methodology, *Journal of Environmental Sciences,* **2010**, **22** (8), 1281-1289;
18. Ferreira, S.C., Bruns, R.E., Ferreira, H.S., Matos, G.D., David, J.M., Brandao, G.C., Dos Santos, W.N.L.: Box-Behnken design: an alternative for the optimization of analytical methods, *Analytica Chimica Acta,* **2007**, **597** (2), 179-186;
19. Wang, J.P., Chen, Y.Z., Wang, Y., Yuan, S.J., Yu, H.Q.: Optimization of the coagulation-flocculation process for pulp mill wastewater treatment using a combination of uniform design and response surface methodology, *Water Research,* **2011**, **45** (17), 5633-5640;
20. Eslami, A., Nasseri, S., Yadollahi, B., Mesdaghinia, A., Vaezi, F., Nabizadeh, R., Nazmara, S.: Photocatalytic degradation of methyl tert-butyl ether (MTBE) in contaminated water by ZnO nanoparticles, *Journal of Chemical Technology and Biotechnology,* **2008**, **83** (11), 1447-1453;
21. Kaneco, S., Li, N., Itoh, K., Katsumata, H., Suzuki, T., Ohta, K.: Titanium dioxide mediated solar photocatalytic degradation of thiram in aqueous solution: Kinetics and mineralization, *Chemical Engineering Journal,* **2009**, **148** (1), 50-56;
22. Nikazar, M., Gholivand, K., Mahanpoor, K.: Photocatalytic degradation of azo dye Acid Red 114 in water with TiO_2 supported on clinoptilolite as a catalyst, *Desalination,* **2008**, **219** (1-3), 293-300;
23. Tonga, T., Zhanga, J., Tiana, B., Chena, F., Heb, D.: Preparation of Fe^{3+}-doped TiO_2 catalysts by controlled hydrolysis of titanium alkoxide and study on their Photocatalyticactivity for methyl orange degradation, *Journal of Hazardous Materials,* **2008**, **155** (3), 572-579.